Indonesian Journal of Chemical Research

http://ojs3.unpatti.ac.id/index.php/ijcr Indo. J. Chem. Res., 14 (2), 199-205, 2026

Synthesis and Characterization of Citrate-Associated Calcium Materials from Blood Clam (*Anadara granosa*) Shells

Azmalaeni Rifkah Ansyarif[1*], Andriani Usman[2], Andi Nuraeni[3], Nur Zyalsabilah As Shahrah[1]

[1]Department of Chemistry, Syekh Yusuf Al Makassari University, Gowa, BTN Andi Tonro Permai Block A 22/5, Gowa Regency, South Sulawesi

[2]Environmental Engineering Program, Syekh Yusuf Al Makassari University of Gowa, BTN Andi Tonro Permai Block A 22/5, Gowa Regency, South Sulawesi

[3]Chemistry Program, Faculty of Science and Technology, Sipatokkong Mambo University, Jl. Wahidin Sudirohusodo No. 75, Macanang, Tanete Riattang Barat Subdistrict, Bone Regency, South Sulawesi

[*]*Corresponding Author: azmalaenira@usy.ac.id*

Received: August 2026
Received in revised: September 2026
Accepted: September 2026
Available online: September 2026

Abstract

Blood clam shell waste is a source of biogenic calcium with the potential to be developed into calcium-based materials. This study synthesized nanocalcium using citrate as a coating agent from blood clam shells and evaluated its functional groups, morphology, and particle size distribution. The shells were cleaned, dried at 150 °C for 1 hour, ground, calcined at 1000 °C for 5 hours, hydrated, reacted with citric acid monohydrate at a 1:2 molar ratio via magnetic stirring and ultrasonication at 40 kHz for 30 minutes, aged for 24 hours, and then freeze-dried. FTIR analysis of calcium oxide (CaO) showed O–H bands at 3643.53–3383.14 cm^{-1} and Ca–O vibrations at 553.57 and 397.34 cm^{-1}. After citrate treatment, C–H bands at 2918.30 and 2854.65 cm^{-1} as well as carbonyl/carboxylate bands at 1743.65, 1707.00, 1587.42, 1431.18, and 1392.61 cm^{-1} indicate the presence of citrate and its coordination with Ca2+. SEM revealed irregular micrometer-scale agglomerates and a rough surface. PSA yielded an average size of 56.08 nm, a peak at 53.25 nm, D10/D50/D90 values of 39.29/53.38/72.75 nm, and a polydispersity index of 0.059.

Keywords: Anadara granosa, calcium citrate, shell waste processing, FTIR, SEM, particle size distribution

INTRODUCTION

Oyster shells are a potential natural source of calcium because their calcium carbonate content can be converted into CaO through calcination. Blood oyster shells (Anadara granosa) are primarily composed of the aragonite phase, and thermal treatment alters their structure and reactivity (Siriprom et al., 2022). The utilization of these shells has been developed for the production of calcium titanate and other calcium compounds, while simultaneously reducing the burden of coastal solid waste (Ardiansah A et al., 2024; Seesanong et al., 2023).

Biomineral waste, including oyster shells and eggshells, is a potential natural source of calcium because its high calcium carbonate content can be converted into CaO through calcination (Usman et al., 2020). Calcination of $CaCO_3$ produces calcium oxide (CaO) determines the degree of conversion, the crystallite size, and the morphology of shell-based materials (Suwannasingha et al., 2022). CaO derived from eggshells also possesses surface properties that facilitate interactions with surrounding ions or compounds (Karim et al., 2025). The CaO formed is hygroscopic, so it readily hydrates to form $Ca(OH)_2$and undergoes recarbonation during handling in air (Chong et al., 2023; Mostafa et al., 2023). Physicochemical characteristics are used to identify functional groups and chemical interactions, while SEM analysis is employed to determine morphology and agglomeration (Nurhana et al., 2025).

Particle size reduction is one approach to increasing the specific surface area and improving the dispersion of calcium-based materials, thereby potentially enhancing their reactivity and effectiveness. Various biogenic sources in Indonesia have been developed as sources of nano-sized calcium, through the release of CO_2. The calcination temperature with particle characteristics that are influenced by the type of raw material and the

synthesis method. Nanocalcium derived from six types of fish bones has been reported to have particle sizes ranging from 87.37 to 281.4 nm (Kusumawati et al., 2022; Rifkah Ansyarif et al., 2025), whereas the use of parang fish bones produces nanocalcium with a size of approximately 62 nm (Hayati et al., 2025). Among other biogenic sources, chicken bones synthesized into calcium citrate yielded a particle size of 524.1 nm (Prayitno et al., 2025). Furthermore, the precipitation of calcium lactate from eggshells indicates that the use of organic acids also has the potential to produce nano-sized calcium materials (Prayitno et al., 2021). These findings demonstrate that the selection of calcium sources and types of organic acids, as well as the control of synthesis conditions, are critical factors in determining the characteristics and particle size of calcium materials.

Citric acid has three carboxyl groups that can coordinate with Ca2+and simultaneously influence nucleation, crystal growth, and agglomeration. Recent research on blood clam shells shows that the concentration of citric acid determines the formation of the hydrated or anhydrous calcium citrate phase (Chanwetprasat et al., 2025).

FTIR characterization generally reveals changes in the carboxylate bands, but the chemical formula and crystal phase cannot be determined by FTIR alone (An et al., 2022; Wang et al., 2024). The use of ultrasonication and a freeze dryer can support the formation and stabilization of chelated calcium materials (Maming et al., 2023). Furthermore, the complexation of Ca2+ions with chelating agents can also be confirmed through a combination of FTIR, SEM, and AAS analyses (Ariesta et al., 2026).

Research integrating calcination-hydration, citrate chelation, sonication, and FTIR, SEM, and PSA evaluations of calcium derived from Anadara granosa shells remains limited. This study aims to synthesize calcium nanoparticles using citric acid as a chelating agent and to characterize their functional groups, morphology, and particle size distribution. Its novelty lies in the use of a calcium precursor obtained by calcining locally sourced shells, followed by a citrate chelation process using ultrasonication and a freeze dryer.

METHODOLOGY

Materials and Instrumentals

The materials used included blood clam shells (*Anadara granosa*), citric acid ($C_6H_8O_7$), and distilled water (H_2O). The main equipment consisted of a Kirin oven, a Thermo Scientific furnace, a grinder, a hotplate stirrer, a magnetic stirrer, an ultrasonic bath (ultrasonic cleaner), and a freeze dryer. Characterization was performed using a Shimadzu FTIR (Fourier Transform Infrared) of the IRPrestige type, a JEOL SEM (Scanning Electron Microscope) of the JCM6000Plus type, and a HORIBA Scientifix Sz-100 PSA (particle size analyzer).

Shell Preparation and Calcination

The shells are sorted and washed until all adhering impurities are removed, then dried. The dried samples are mechanically crushed and ground into a powder. The powder is dried in an oven at 150 °C for 1 hour, then calcined in a furnace at 1000 °C for 5 hours. The calcined product is cooled and stored in a sealed container to limit hydration and carbonation by air. The main reaction expected is:

$$CaCO_{3(s)} \rightarrow CaO_{(s)} + CO_{2(g)}$$

Hydration of the CaO Precursor

A total of 0.561 g of CaO (±0.0100 mol) from the calcination was placed in a 100 mL beaker; 25 mL of distilled water was added while stirring with a magnetic stirrer. The mixture was stirred for 30 minutes at room temperature until a homogeneous $Ca(OH)_2$ suspension formed. The reaction can be written as the following equation:

$$CaO_{(s)} + H_2O_{(l)} \rightarrow Ca(OH)_{2(s)}$$

Based on the initial number of moles of CaO and the 1:1 stoichiometry of hydration, the nominal amount of $Ca(OH)_2$formed is approximately 0.0100 mol; thus, the precursor concentration, assuming a volume of 25 mL, is approximately 0.400 mol/L.

After the hydration process, the beaker was covered with aluminum foil to minimize contact with $CO_2$and reduce the likelihood of $CaCO_3$ formation. The resulting hydration suspension was then used directly in the mixing stage with the chelating agent without prior drying.

Mixing with Citric Acid

A total of 4.203 g (0.0200 mol) of citric acid was dissolved in 25 mL of distilled water to yield a concentration of 0.800 mol/L. The nominal molar ratio of Ca to citric acid used is 1:2. This ratio was chosen to promote the interaction of Ca2+ions with carboxylate groups and to aid in the formation and stabilization of calcium citrate complexes.

The $Ca(OH)_2$ suspension was then slowly added to the citric acid solution while stirring with a magnetic stirrer at 600 rpm. Combine stirring with an ultrasonic bath (ultrasonic cleaner) at a frequency of

40 kHz for 30 minutes, with an ultrasonic power of approximately 60–120 W, and a voltage of 220–240 V. Place the 100 mL beaker in the center of the ultrasonic bath. Afterward, let it stand for 24 hours at room temperature, then proceed with the drying process using a freeze dryer.

Verification of the precursor was performed using FTIR to detect the presence of O-H and Ca-O vibrations. This verification serves as supporting evidence for the formation of the hydrated precursor.

Characterization and Data Analysis

The FTIR spectra of the calcined precursor and the citrate-associated product were recorded in the range of approximately 4000–350 cm^{-1}. The powder morphology was observed using SEM under high-vacuum conditions, with a secondary electron detector, an acceleration voltage of 15 kV, and magnifications of 100x, 270x, and 1000x. Particle size distribution was determined using PSA. The FTIR and SEM data were analyzed descriptively. The PSA data are presented as mean size, distribution peak, D10, D50, D90, and polydispersity index (PI).

RESULTS AND DISCUSSION

Characteristics of the Calcined Precursor

The FTIR spectrum of the calcined precursor (Figure 1) shows a sharp band at 3643.53 $cm^{-1}$and bands at 3562.52, 3441.01, and 3383.14 cm^{-1}, which are associated with the O–H stretching of $Ca(OH)_2$ and adsorbed water. These findings are consistent with the hygroscopic nature of CaO, which readily reacts with moisture upon removal from the furnace. Low-frequency bands at 553.57 and 397.34 cm^{-1} support the presence of Ca-O vibrations (Chong et al., 2023; Mostafa et al., 2023).

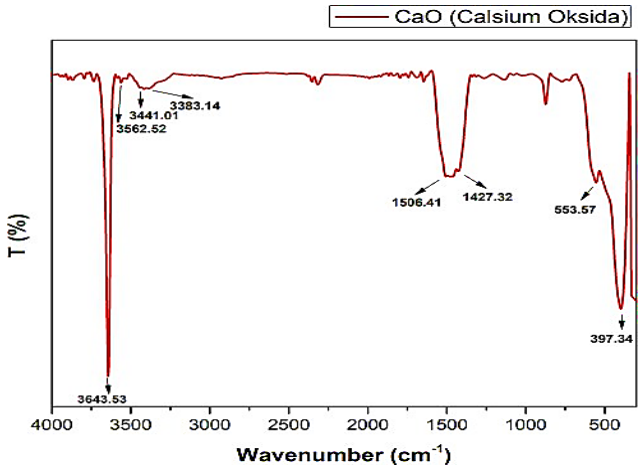

Figure 1. FTIR spectrum of the calcium precursor obtained from the calcination of blood clam shells.

The bands at 553.57 and 397.34 indicate the Ca-O vibration region. This is supported by a study showing that the band in the 550 cm^{-1} region corresponds to the Ca-O vibration. Therefore, the bands in this region indicate the presence of Ca-O bonds in the calcination product (Mostafa et al., 2023).

Spectroscopic Evidence of Calcium-Citrate Interactions

Treatment with citric acid produced noticeable changes in the FTIR spectrum (Figure 2). The broadened O-H bands at 3446.79, 3385.07, and 3298.28 cm^{-1}indicate hydrogen-bonded environments of the citric acid hydroxyl groups and bound water. The bands at 2918.30 and 2854.65 cm^{-1} originate from the C–H vibrations of the organic components. The appearance of C=O bands at 1743.65 and 1707.00 cm^{-1} indicates the continued presence of protonated carboxylate groups.

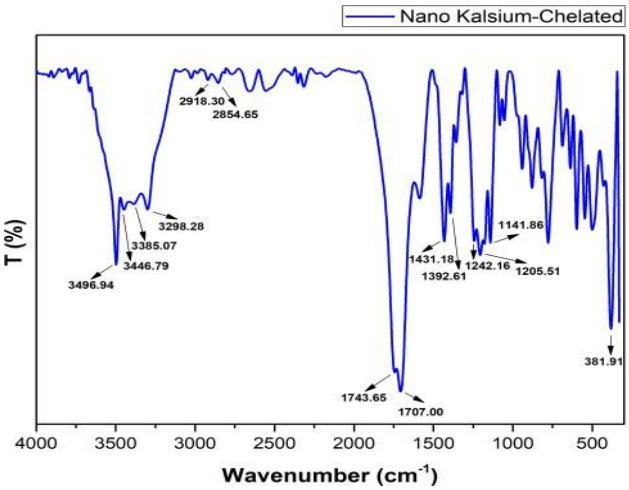

Figure 2. FTIR spectrum of nanocalcium after citric acid treatment

The band at 1587.42 $cm^{-1}$is associated with the asymmetric stretching of COO^-, and the bands at 1431.18 and 1392.61 $cm^{-1}$with the symmetric stretching of the carboxylate group. The separation between the 1587.42 and 1392.61 cm^{-1} bands, which is 194.81 cm^{-1}, indicates a change in the carboxylate coordination environment, but is not sufficient to determine its coordination geometry. The bands at 1242.16, 1205.51, and 1141.86 $cm^{-1}$are associated with C–O vibrations. The presence of carbonyl, carboxylate, and C–O bands indicates the existence of functional groups associated with citrate in the synthesis product. This pattern is consistent with reports on calcium citrate from seashells, which exhibit both asymmetric and symmetric COO– bands

as well as citrate C–O bands (Chanwetprasat et al., 2025). Other studies on calcium chelates have also demonstrated the involvement of carboxylate and C-O groups in Ca2+coordination (An et al., 2022; Zhong et al., 2023).

FTIR analysis cannot be used to determine the identity of the crystalline phase; XRD analysis is required to confirm the formation of a crystalline phase.

Table 1. Major FTIR functional groups of citrate chelating precursors and products

Sample	Band (cm^{-1})	Functional Group
CaO	3643.53–3383.14	O-H; hydration/adsorbed water
CaO	1506.41; 1427.32	Residual carbonate/recarbonation
CaO	553.57; 397.34	Ca-O Vibrations
Chelated Nano-Calcium	3446.79–3298.28	O-H and hydrogen bonds
Chelated Nano-Calcium	2918.30; 2854.65	C-H Stretch
Chelated Nano-Calcium	1743.65; 1707.00	C=O from -COOH
Chelated Nano-Calcium	1587.42; 1431.18; 1392.61	COO- Stretch
Chelated Nano-Calcium	1242.16; 1205.51; 1141.86	C-O strain in citrate

Morphology and Agglomeration

The SEM micrograph (Figure 3) shows an irregular morphology with a tendency to form agglomerates. At magnifications of x100 and x270, agglomerates ranging in size from tens to hundreds of micrometers are visible. At x1000, the agglomerates are composed of smaller fragments, but the boundaries of the primary particles, which are tens of nanometers in size, cannot yet be clearly resolved. This indicates that the SEM observations under the conditions used primarily depict the morphology of dry powder agglomerates, rather than the size of the primary particles. Irregular morphology and a tendency to agglomerate have also been reported in chicken bone nanocalcium citrate and other calcium citrate nanoparticles (Oopkaew et al., 2024; Prayitno et al., 2025).

Agglomeration can be triggered by high surface energy, hydrogen bonding, interfacial ionic interactions, and particle coalescence during the freeze-drying process. In peptide-based calcium chelates, structural changes and aggregation following complex formation have also been observed via SEM and particle size analysis (Zhong et al., 2023b). The SEM results obtained in this study only examined the morphology of the material in a dry state; therefore, the primary particles may appear as larger agglomerates. The SEM data obtained cannot be used to determine the primary particle size, which requires characterization using TEM.

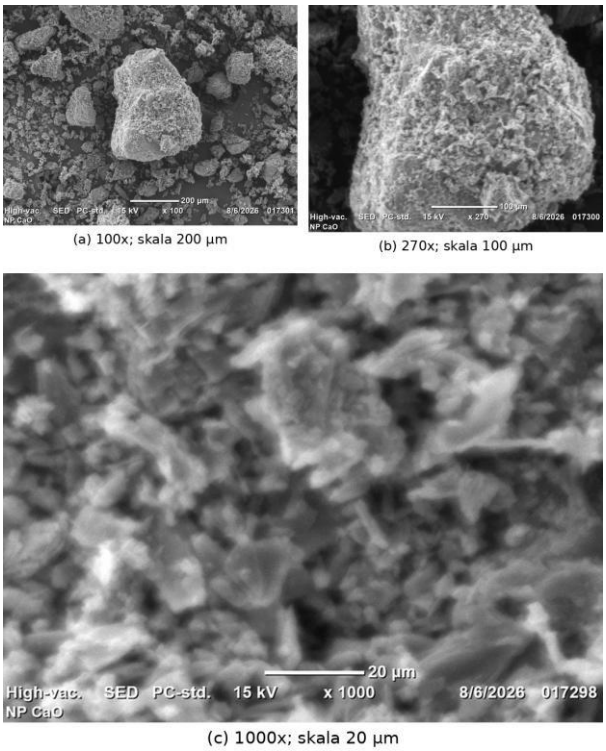

(a) 100x; skala 200 µm (b) 270x; skala 100 µm

(c) 1000x; skala 20 µm

Figure 3. Morphology of chelated calcium citrate nanopowder at magnifications of (a) 100x, (b) 270x, and (c) 1000x

Particle Size Distribution

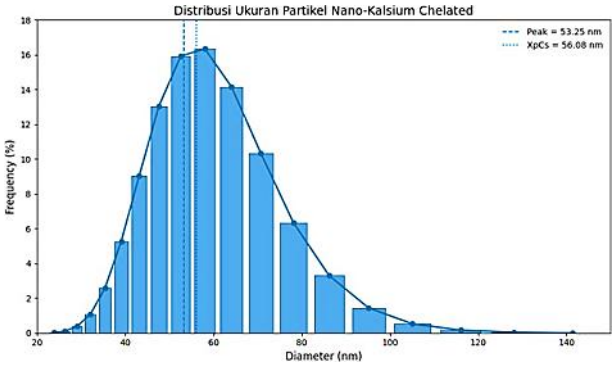

Figure 4. Particle size distribution of chelated citrate nano-calcium based on PSA

PSA yielded an average size of 56.08 nm with a distribution peak at 53.25 nm. The D10, D50, and D90 values were 39.29, 53.38, and 72.75 nm,

respectively (Table 2). The PI value obtained using the PSA instrument is 0.059. The closeness of the mean size, peak, and D50 values indicate a consistent distribution center. A PI value of 0.059 indicates a narrow distribution, while the calculated span of 0.627 illustrates the relative width of the D10–D90 distribution.

Table 2. Particle size distribution parameters

Parameter	Value
Mean	56.08 nm
Peak	53.25 nm
D10	39.29 nm
D50	53.38 nm
D90	72.75 nm
PI	0.059
Span	0.627

The size of 56.08 nm is smaller than the 62 nm observed in nanocalcium from parang fish bones (Hayati et al., 2025), the range of 87.37–281.4 nm in nanocalcium from fish bones (Kusumawati et al., 2022), and 524.1 nm in chicken bone citrate nanocalcium (Hadi Prayitno et al., 2025). Usman et al. (2020) also obtained nanometer-sized CaO from green mussel and batik mussel shells, with sizes of 88.76 and 96.67 nm, respectively. These comparisons must be interpreted with caution because the material composition, instrument principles, dispersion media, and sample pretreatment differ. Research on the optimization of $CaCO_3$ nanoparticles also indicates that reactant concentration and mixing conditions significantly determine monodispersity (Persano et al., 2022). Ultrasonic assistance can improve mass transfer and dispersion during the formation of chelated calcium systems (Qu et al., 2024).

The discrepancy between micrometer-sized agglomerates observed by SEM and nanometer-sized particles measured by PSA is not contradictory. SEM examines dry powders that have undergone agglomeration, whereas PSA measures the dispersed particle population. However, without TEM or high-resolution SEM, PSA data do not directly confirm the primary particle diameter. Furthermore, the presence of a strong -COOH band indicates the need for washing and optimization of the reactant ratio to reduce the likelihood of citric acid residue. Acid concentration, stirring time, and crystallization conditions have been reported to influence the phase, morphology, and properties of calcium-based materials (Chanwetprasat et al., 2025; Wang et al., 2024; Wijayanti et al., 2024; Yan et al., 2023).

Limitations and Implications

A major limitation of this study is the lack of XRD for phase identification, EDX/ICP-OES for verifying calcium content, TGA/DSC for determining the degree of hydration, zeta potential for dispersion stability, and high-resolution TEM/SEM for primary particle size. Instrumental conditions and the number of replicates also need to be fully documented. Nevertheless, the combination of FTIR changes and PSA distribution provides consistent preliminary evidence that the citrate treatment produces nano-sized calcium materials with a relatively narrow distribution. Before being applied as a food fortifier, the composition, purity, solubility, safety, stability, and in vitro bioaccessibility must be tested.

CONCLUSION

Blood clam shells were successfully processed into citrate-associated calcium powder with a dry mass of 2.18 g. FTIR analysis showed a transition from the hydrated/carbonated CaO precursor to a material containing citrate groups, as indicated by the C-H, C=O, COO-, and C-O bands. SEM revealed an irregular morphology and agglomeration under dry conditions. PSA analysis yielded an average size of 56.08 nm, a peak at 53.25 nm, D10/D50/D90 values of 39.29/53.38/72.75 nm, and a PI of 0.059. These results support the formation of a narrowly distributed calcium citrate-associated material; however, the phase identity and primary particle size still need to be confirmed through XRD, compositional analysis, and high-resolution microscopy before claims and applications as a food fortifier can be further developed.

ACKNOWLEDGMENT

The authors would like to thank the Directorate of Research and Community Service, Ministry of Higher Education, Science, and Technology of the Republic of Indonesia for funding through the 2026 Early-Career Faculty Research Program.

REFERENCES

An, J., Zhang, Y., Ying, Z., Li, H., Liu, W., Wang, J., & Liu, X. (2022). The Formation, Structural Characteristics, Absorption Pathways and Bioavailability of Calcium–Peptide Chelates. *Foods*, *11*(18), 2762.

Ardiansah A, Pratiwi, D. E., J, Muh. A. A., Utami, H. H., & Malau, A. (2024). Sintesis Kalsium Titanat ($CaTiO_3$) dari Cangkang Kerang Darah (Anadara

granosa Linn) dengan Metode Hidrotermal. *Journal of Chemical Process Engineering*, *9*(1), 11–18.

Ariesta, A. S., Zulfikar, M. A., & Patah, A. (2026). Tailoring MOF-303 with CaCl2 and Graphite: A Promising Material for Atmospheric Water Capture. *Indonesian Journal of Chemical Research*, *14*(1), 88–95.

Chanwetprasat, P., Seangarun, C., Seesanong, S., Boonchom, B., Laohavisuti, N., Boonmee, W., & Rungrojchaipon, P. (2025). Effect of Citric Acid Concentration on the Transformation of Aragonite CaCO3 to Calcium Citrate Using Cockle Shells as a Green Calcium Source. *Materials*, *18*(9), 2003.

Chong, N. S., Nwobodo, I., Strait, M., Cook, D., Abdulramoni, S., & Ooi, B. G. (2023). Preparation and Characterization of Shell-Based CaO Catalysts for Ultrasonication-Assisted Production of Biodiesel to Reduce Toxicants in Diesel Generator Emissions. *Energies*, *16*(14), 5408.

Hadi Prayitno, A., Syafi'ul Umam, M., Ridho, M. R., Safitri, A. R., & Roihan, N. A. (2025). Characteristics and Antibacterial Activity of ZnO Nanoparticle Fortified Probiotic Yogurt Characterisation of Nano-Calcium Citrate from Waste Broiler Chicken Bones Synthesized Using Lime as a Novel Food Supplement. *Bulletin of Animal Science*, *3*(49), 187–193.

Hayati, F., Pranoto, Y., & Triwitono, P. (2025). Bioavailability of Nano-calcium from Parang Fishbone Extracted with Alkaline Solvent at Varying Ratio of NaOH and Extraction Time. *Indonesian Food and Nutrition Progress*, *22*(1), 13.

Karim, K. R., Firnanelty, F., & Fadhilah, N. (2025). Adsorption of Inorganic and Organic Waste of Chemistry Laboratory by Using Eggshell-based CaO. *Indonesian Journal of Chemical Research*, *13*(2), 168–175.

Kusumawati, P., Triwitono, P., Anggrahini, S., & Pranoto, Y. (2022). Nano-calcium Powder Properties from Six Commercial Fish Bone Waste in Indonesia. *Squalen Bulletin of Marine and Fisheries Postharvest and Biotechnology*, *17*(1), 1–12.

Maming, M., Mubakira, F., Raya, I., Musa, B., Anshar, A. M., Mayasari, E., Hala, Y., Kasim, S., Andi, I. L., Alam, G., Usman, A. N., Hasmawati, H., Hasri, H., Usman, A., & Irfandi, R. (2023). Fabrication and analysis of nano-hydroxyapatite [Ca10(PO4)6(OH)2] composites with collagen derived from eggshells through freeze-drying. *Journal of Medicinal and Pharmaceutical Chemistry Research*, *5*(12), 1173–1193.

Mostafa, F. A., Gad, A. N., Gaber, A.-A. M., & Abdel-Wahab, A.-M. A. (2023). Preparation, Characterization and Application of Calcium Oxide Nanoparticles from Waste Carbonation Mud in Clarification of Raw Sugar Melt. *Sugar Tech*, *25*(2), 331–338.

Nurhana, E. A., Perdani, M. S., Umam, H. I., Fadilla, A. D., & Sitanggang, C. O. (2025). Physicochemical Characterization and Recyclability of CaO/SiO_2 Catalysts Derived from Eggshell and Rice Husk for Biodiesel Application. *Indonesian Journal of Chemical Research*, *13*(2), 176–185.

Oopkaew, L., Injongkol, Y., Rimsueb, N., Mahalapbutr, P., Choowongkomon, K., Hadsadee, S., Rojanathanes, R., & Rungrotmongkol, T. (2024). Targeted Therapy with Cisplatin-Loaded Calcium Citrate Nanoparticles Conjugated with Epidermal Growth Factor for Lung Cancer Treatment. *ACS Omega*, *9*(24), 25668–25677.

Persano, F., Nobile, C., Piccirillo, C., Gigli, G., & Leporatti, S. (2022). Monodisperse and Nanometric-Sized Calcium Carbonate Particles Synthesis Optimization. *Nanomaterials*, *12*(9), 1494.

Prayitno, A. H., Umam, M. S., Ridho, M. R., Safitri, A. R., & Roihan, N. A. (2025). Characterisation of Nano-Calcium Citrate from Waste Broiler Chicken Bones Synthesized Using Lime as a Novel Food Supplement. *Buletin Peternakan*, *49*(3), 187.

Qu, W., Feng, Y., Xiong, T., Qayum, A., & Ma, H. (2024). Preparation, structural and functional characterization of corn peptide-chelated calcium microcapsules using synchronous dual frequency ultrasound. *Ultrasonics Sonochemistry*, *102*, 106732.

Rifkah Ansyarif, A., Bahar, H., Fatmasari, R., & Syekh Yusuf Al Makassari Gowa, U. (2025). Karakterisasi Kimia Dan Mikrobiologi Kerupuk Ikan Bandeng (Chanos chanos): Analisa Gizi Dan Mutu Produk untuk Aplikasi Industri. *Katalis: Jurnal Penelitian Kimia Dan Pendidikan Kimia*, *8*(2), 2721–2902.

Seesanong, S., Seangarun, C., Boonchom, B., Phutphat, S., Rungrojchaipon, P., Montri, N., Thompho, S., Boonmee, W., & Laohavisuti, N. (2023). Efficient, Green, and Low-Cost Conversion of Bivalve-Shell Wastes to Value-

Added Calcium Lactate. *ACS Omega*, *8*(30), 27044–27055.

Siriprom, W., Phae-ngam, W., & Kohmun, K. (2022). Effects of temperature and moisture on phase transition of Anadara granosa shells. *Materials Today: Proceedings*, *65*, 2362–2368. https://doi.org/10.1016/J.MATPR.2022.05.345

Suwannasingha, N., Kantavong, A., Tunkijjanukij, S., Aenglong, C., Liu, H.-B., & Klaypradit, W. (2022). Effect of calcination temperature on structure and characteristics of calcium oxide powder derived from marine shell waste. *Journal of Saudi Chemical Society*, *26*(2), 101441.

Usman, M. R., Nabila, R., & Hakiki, L. N. (2020). Ekstraksi Kalsium dari Cangkang Kerang Hijau (Perna viridis L.) dan Kerang Batik (Paphia undulata B.) dengan Metode Kalsinasi sebagai Sediaan Effervescent. *Indonesian Journal of Chemical Research*, *8*(2), 101–107.

Wang, Z., Zhao, Y., Yang, M., Wang, Y., Wang, Y., Shi, C., Dai, T., Wang, Y., Tao, L., & Tian, Y. (2024). Glycated Walnut Meal Peptide–Calcium Chelates: Preparation, Characterization, and Stability. *Foods*, *13*(7), 1109.

Wijayanti, Ph. D. I., Agustini, T. W., Swastawati, F., Anggo, A. D., & Afifah, D. N. (2024). Optimization of Catfish (Pangasius sp) Bone Bio-calcium Production with Different Concentrations of Citric Acid and Stirring Time Using the Response Surface Method (RSM) Approach. *Squalen Bulletin of Marine and Fisheries Postharvest and Biotechnology*, *19*(2), 81–95.

Yan, H., Liu, Y., Peng, H., Li, K., Li, C., Jiang, S., Chen, M., Han, D., & Gong, J. (2023). Improving calcium citrate food functions through spherulitic growth in reactive crystallization and a mechanism study. *Food Chemistry*, *404*, 134550.

Zhong, Y., Zhou, Y., Ma, M., Zhao, Y., Xiang, X., Shu, C., & Zheng, B. (2023a). Preparation, Structural Characterization, and Stability of Low-Molecular-Weight Collagen Peptides–Calcium Chelate Derived from Tuna Bones. *Foods*, *12*(18), 3403.

Zhong, Y., Zhou, Y., Ma, M., Zhao, Y., Xiang, X., Shu, C., & Zheng, B. (2023b). Preparation, Structural Characterization, and Stability of Low-Molecular-Weight Collagen Peptides–Calcium Chelate Derived from Tuna Bones. *Foods*, *12*(18), 3403.